

Quantumswitched heterojunction bipolar transistor

Ming C. Wu and W. T. Tsang

Citation: [Applied Physics Letters](#) **55**, 1771 (1989); doi: 10.1063/1.102214

View online: <http://dx.doi.org/10.1063/1.102214>

View Table of Contents: <http://scitation.aip.org/content/aip/journal/apl/55/17?ver=pdfcov>

Published by the [AIP Publishing](#)

Articles you may be interested in

[Quantum-well-base heterojunction bipolar light-emitting transistor](#)

Appl. Phys. Lett. **84**, 1952 (2004); 10.1063/1.1669071

[Quantumswitched heterojunction bistable bipolar transistor by chemical beam epitaxy](#)

Appl. Phys. Lett. **57**, 150 (1990); 10.1063/1.103968

[Achievement of high gain in a multiple quantum channel lateral heterojunction bipolar transistor](#)

Appl. Phys. Lett. **56**, 1670 (1990); 10.1063/1.103112

[Electroluminescence from a heterojunction bipolar transistor](#)

Appl. Phys. Lett. **45**, 537 (1984); 10.1063/1.95306

[Graded collector heterojunction bipolar transistor](#)

Appl. Phys. Lett. **44**, 105 (1984); 10.1063/1.94540



AIP | Journal of
Applied Physics

Journal of Applied Physics is pleased to
announce **André Anders** as its new Editor-in-Chief

Quantum-switched heterojunction bipolar transistor

Ming C. Wu and W. T. Tsang

AT&T Bell Laboratories, Murray Hill, New Jersey 07974

(Received 12 June 1989; accepted for publication 25 August 1989)

We propose and demonstrate a negative differential resistance transistor—the quantum-switched heterojunction bipolar transistor (QSHBT). It has the highest current peak-to-valley ratio ever reported at room temperature (15 in an InGaAs/InP QSHBT). More important, the switching and peak-to-valley ratio can be controlled by a base current injected electronically or optically. For example, a peak current as high as 72 mA or 2.9 kA/cm² can be controlled by either a few microamperes of base current or a few microwatts of optical signal. A gain of peak current of 8650 at room temperature is obtained. The present device is grown by chemical beam epitaxy.

Three-terminal negative differential resistance (NDR) devices have great potentials for applications in logic, memory, and microwave circuits. They are more flexible than the two-terminal devices because they have one more degree of freedom in control. Previously proposed and demonstrated NDR transistors incorporated a resonant tunneling double-barrier (RTDB) structure either in the base or between the base/emitter junction of a bipolar or a hot-electron transistor.¹⁻⁵ Some unipolar NDR field-effect transistors (FETs) with RTDB in the gate or between gate and source were also demonstrated.^{6,7} So far most of the devices operate at 77 K. The best current peak-to-valley ratios (PVRs) reported to date are 7 (100 K) in a GaAs/GaAlAs resonant tunneling bipolar transistor (RBT),³ 15 (77 K) in a GaAs/GaAlAs resonant tunneling hot-electron transistor (RHET),⁴ and 3.5 (300 K) in an InAlAs/InGaAs RBT.⁵ In this letter, we report the performance of a novel NDR transistor, the quantum-switched heterojunction bipolar transistor (QSHBT). It has a current PVR as high as 15, the highest value ever reported, a peak current of 72 mA (3 kA/cm²), and a peak current gain of 8650 at room temperature. More important, for the first time, the switching and the peak-to-valley ratio can be controlled by the base current as small as a few microamperes. The control is also possible with an optical light signal of a few microwatts. The large current-driving capability makes this device particularly suitable for driving a laser diode or a light-emitting diode (LED), thus an all-optical switch or regenerator can be realized in this structure.

The QSHBT uses a totally new principle to achieve NDR. A schematic diagram is shown in Fig. 1. The collector layer in a conventional heterojunction bipolar transistor is replaced with a 40-period undoped superlattice. The material is prepared by chemical beam epitaxy (CBE) on an *n*⁺-InP substrate. The details of the growth process were given in Ref. 8. The sequence of the grown layers is as follows: a 3000-Å-thick *n*⁺-InP collector, a 300-Å-thick undoped InP setback layer, a 40-period superlattice with 100-Å-thick InGaAs wells and 100-Å-thick InP barriers all undoped, a 200-Å-thick undoped InP setback layer, a 300-Å-thick *n*⁻-InP layer ($N_D = 3 \times 10^{16}$ cm⁻³), a 500-Å-thick *n*⁻-InGaAs transition layer ($N_D = 3 \times 10^{16}$ cm⁻³), a 1500-Å-thick *p*⁺-InGaAs base ($N_A = 2 \times 10^{18}$ cm⁻³), a 5000-Å-thick *n*-InP emitter ($N_D = 5 \times 10^{17}$ cm⁻³), and finally a 2000-Å-thick *n*⁺-InGaAs cap layer.

The *n*⁻-doped part of the InGaAs base is to reduce the collector potential barrier in the ON state,⁹ as will be discussed in more detail later. After growth, an emitter mesa of area 2.5×10^{-5} cm² was selectively etched to the InGaAs base layer. Then Ni/Ge/Au/Ag/Au and AuBe/Ti/Au were evaporated for emitter and base contacts, respectively. The device is isolated by mesa etching through the base and the multiquantum wells. Typical mesa area is 3.4×10^{-4} cm². After backside evaporation for the collector contact, the device is sintered at 400 °C for 10 s.

A striking feature is observed in the common emitter current voltage (*I*-*V*) characteristics of the QSHBT, as shown in Fig. 2. The different traces are for different base currents *I*_B, starting from 6 μA and increasing with a 4 μA step. At around 2.7 V, the *I*_C corresponding to the *I*_B = 6 μA trace switches from a high-current state back to a low-current state, producing a negative differential resistance behavior. As *I*_B increases, *I*_C switches at higher current. At *I*_B = 22 μA, the current switches from 72 to 4.7 mA. The current peak-to-valley ratio of 15 is the highest value ever reported for any kind of NDR transistor at room temperature. The gain of the peak current β_{peak} , defined as $dI_{C\text{peak}}/dI_B$, is as high as 8650 at *I*_C = 60 mA and *V*_{CE} = 3.4 V. The switching behavior is, to some extent, dependent on external circuit parameters. We would like to point out that no effort has yet been made to optimize the structure. Even better performance is very likely with further device optimization.

A very important new feature of the QSHBT is that the PVR is controllable by adjusting the base current in the microampere range. Such low bias current also suggests that the QSHBT can be switched optically. Indeed, similar common-emitter *I*-*V* characteristics were observed by replacing

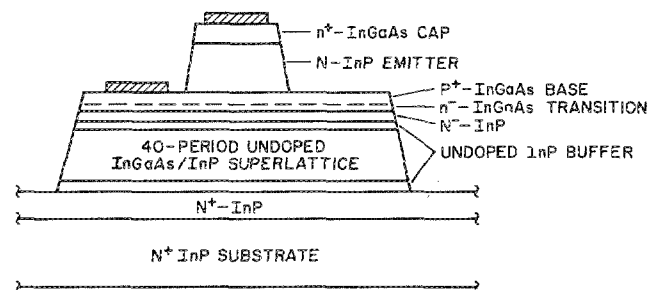


FIG. 1. Schematic structure of the InGaAs/InP QSHBT.

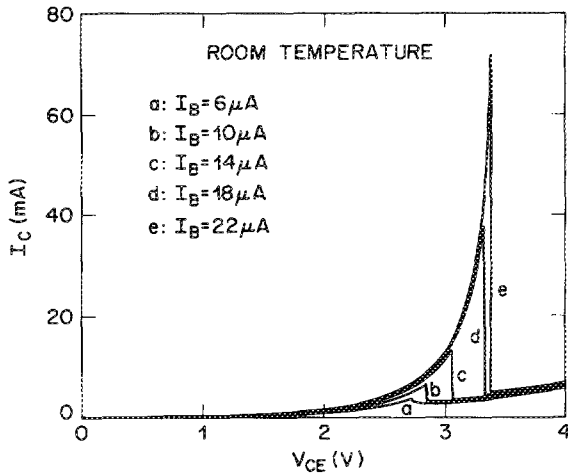


FIG. 2. Common-emitter I - V characteristics of the QSHBT at room temperature. The emitter size is $2.5 \times 10^{-5} \text{ cm}^2$. Large peak-to-valley ratio of I_C can be switched by only a few microamperes of I_B .

the base current with the microscope light above the probe station with different intensities. The high peak current, 72 mA or 2.9 kA/cm^2 , is more than enough to drive a semiconductor laser. The large current PVR will produce a high ON-OFF ratio for the emitted light. Thus, an all-optical switch (flip-flop) with high optical gain or an optical regenerator can be realized with a QSHBT. The laser can be monolithically integrated by growing the laser below the collector.

Furthermore, unlike the previous resonant tunneling devices, the voltage (V_{CE}) at which NDR occurs can be designed to suit particular applications by changing the total thickness (or number of periods) of the superlattice. We also measured separately the ideality factor n of the base-emitter junction with collector open and obtained a value of 1.002. This indicates that the InP/InGaAs heterointerfaces in these devices are of very high quality.

To gain more insight into the device, we also plot the common-emitter I - V curves on a logarithmic scale, together with the base voltage V_{BE} , as shown in Fig. 3. In addition

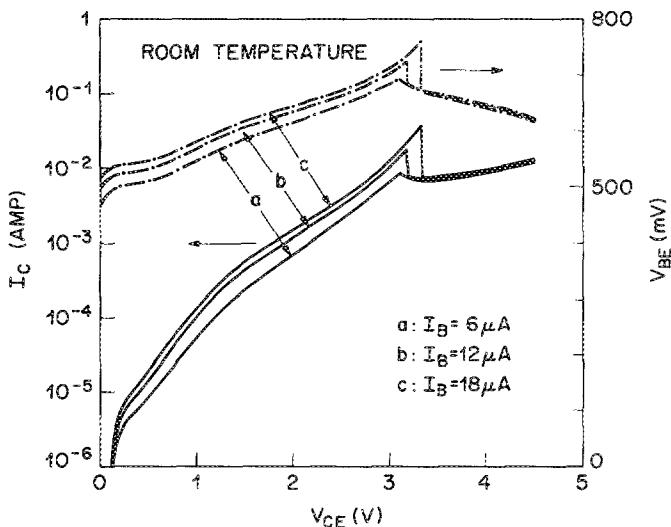


FIG. 3. Base voltage V_{BE} and logarithmic collector current I_C vs collector voltage V_{CE} for QSHBT in common-emitter configuration at room temperature.

to I_C , the behavior of V_{BE} is also very different from conventional transistors. Before I_C switches back to the low-current state, V_{BE} increases with V_{CE} and thus I_C . However, after the switch V_{BE} decreases with I_C . Switching also occurs in V_{BE} when I_C switches. Thus, the two different states for the QSHBT can be described as one having I_C and V_{BE} in phase, and the other with them out of phase. This shows that as I_C is switched, the emitter-base voltage is also readjusted.

We believe that the switching is due to the field reconfiguration in the superlattice region. The above device characteristics can be explained qualitatively with the schematic band diagram shown in Fig. 4. Figure 4(a) shows the band diagram of a QSHBT at low bias voltage ($0.2 \text{ V} < V_{CE} < 1.2 \text{ V}$). In this regime the current conduction is due to thermionic emission (dominant) and ground-state resonant tunneling. The conduction-band edge varies parabolically from the base to the superlattice collector due to the charges trapped in the well. The I_C increases exponentially with V_{CE} because the potential barrier at the base/collector heterointerface is pulled down by V_{CE} slowly. As the voltage increases to the point such that the ground state of the second-to-last well is in resonant with the first excited state of the last well [Fig. 4(b)], a high-field domain is formed near the collector contact. This causes a sudden change in the slope of the $\log(I_C)$ vs V_{CE} curve at $V_{CE} \approx 1.2 \text{ V}$ (see Fig. 3), because now most voltage drops in the high-field domain and the base-collector barrier height become less sensitive to increasing V_{CE} . The superlattice collector differs from a homogeneous-material collector in that space charges can be stored in the quantum wells so that an abrupt high-field do-

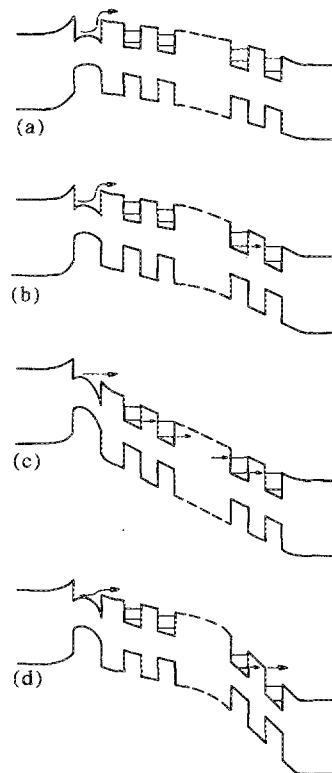


FIG. 4. Schematic band diagrams of the QSHBT at (a) $V_{CE} = 0.2$ - 1.2 V , (b) $V_{CE} = 1.2$ - 2.5 V , (c) peak current ($V_{CE} \approx 3 \text{ V}$), and (d) after switching back to a low current state ($V_{CE} > 3 \text{ V}$).

main can be formed. The field strength in the domain is fixed and is of the order of $F = (E_2 - E_1)/d$, where E_1 and E_2 are the ground-state and the first excited-state energies, respectively, and d is the period of the superlattice. The space charges in the well next to the high-field domain screen the field for the low-field region close to the base. When voltage increases, the high-field domain expands towards the base.

When the high-field domain expands to the base at about $V_{CE} \approx 2.7$ V (note that this voltage depends on the total thickness of the superlattice collector), the space charge in the last well is also depleted and the base-collector barrier lowered substantially. The collector current increases rapidly because the transport efficiency from emitter to collector is almost unity, and the electrons travel through the superlattice by sequential resonant tunneling. This is illustrated in Fig. 4(c). A further increase in V_{CE} will destroy the sequential resonant tunneling condition in the superlattice. As a result, I_C decreases, which in turn triggers the decrease in V_{BE} . The decrease in V_{BE} stimulates a further decrease in I_C . This process continues until it reaches another stable state. The field distribution in the superlattice also changes to another configuration. A high-field domain is again nucleated near the collector side [Fig. 4(d)], corresponding probably to the lineup of the ground state in one well to the continuum state in the adjacent well. The field becomes small again in the superlattice close to the base, where the thermionic current is dominant.

The transport properties of a heterostructure superlattice were first studied by Kazarinov and Suris¹⁰ in 1971 after their initial proposal by Esaki and Tsu¹¹ in 1970. A set of narrow peaks in the current-voltage characteristics, or conductance oscillation, was predicted. Such oscillation has been observed by Esaki and Chang,¹² and later by other groups,¹³⁻¹⁵ even at room temperature.¹³ High-field domain formation discussed was confirmed by optical probing techniques.^{16,17}

The operation of the QSHBT can also be explained phenomenologically as follows. The base current can be written as

$$I_b = I_{b_0} e^{qV_{be}/nkT} + I_c [(1 - \alpha)/\alpha], \quad (1)$$

where I_{b_0} is the reverse leakage current of the base/emitter junction, q is the electron charge, n is the ideality factor, and α is the transport coefficient from emitter to collector. The first term is the hole injection current into the emitter and the second term is the recombination current. In QSHBTs, α is mainly determined by the base-collector potential barrier, which is very sensitive to the field configuration in the superlattice. Using Eq. (1) and the experimental data in Fig. 3, we can find the behavior of α . At low V_{CE} , V_{BE} is small and

recombination current is the dominant base current. Since I_C is very small, this implies that the transport efficiency α is low. Near the peak of I_C , the injection current in Eq. (1) becomes dominant and, therefore, α is very close to unity. This is consistent with the picture of Fig. 4(c). At switching, both I_C and V_{BE} drop, and thus the transport efficiency α decreases from the highest value at the current peak. Beyond the switching point, I_C increases while V_{BE} continues to decrease. The α in this regime is increasing slowly.

In conclusion, we have demonstrated a totally new NDR transistor—the quantum-switched heterojunction bipolar transistor. It has the highest current peak-to-valley ratio ever reported at room temperature, 15. The peak current, as high as 72 mA or 2.9 kA/cm², can be controlled by either a few microamperes of base current or a few microwatts of optical signal. The operation principal of this novel device is believed to be the switching between two internal transistor states, corresponding to different field configurations in the superlattice collector. This new device has great potential as an optoelectronic/all-optical flip-flop, memory, logic gate, or optical regenerator.

The authors would like to thank L. Yang and Y. K. Chen for technical assistance, and R. F. Kazarinov, D. V. Lang, A. Sudbo, and R. Nottenburg for useful discussions.

¹F. Capasso and R. A. Kiehl, *J. Appl. Phys.* **58**, 1366 (1985).

²N. Yokoyama, K. Imaura, T. Mori, S. Hiyamizu, and H. Nishi, *Jpn. J. Appl. Phys.* **24**, L-853 (1985).

³F. Capasso, S. Sen, A. C. Gossard, A. L. Hutchinson, and J. H. English, *IEEE Electron Device Lett.* EDL-7, 573 (1986).

⁴K. Imamura, S. Muto, H. Ohnishi, T. Fujii, and N. Yokoyama, *Electron. Lett.* **23**, 870 (1987).

⁵T. Futatsugi, Y. Yamaguchi, S. Muto, N. Yokoyama, and A. Shibatomi, *IEEE International Electron Device Meeting Technical Digest* (IEEE, Washington, DC, 1987), p. 877.

⁶T. K. Woodward, T. C. McGill, and R. D. Burnham, *Appl. Phys. Lett.* **51**, 451 (1987).

⁷F. Capasso, S. Sen, and A. Y. Cho, *Appl. Phys. Lett.* **51**, 526 (1987).

⁸For a review, see W. T. Tsang, *J. Cryst. Growth* **81**, 261 (1987).

⁹L. M. Su, N. Grote, R. Kaumanns, and H. Schroeter, *Appl. Phys. Lett.* **47**, 28 (1985).

¹⁰R. F. Kazarinov and R. A. Suris, *Sov. Phys. Semicond.* **5**, 707 (1971).

¹¹L. Esaki and R. Tsu, *IBM J. Res. Develop.* **16**, 61 (1970).

¹²L. Esaki and L. L. Chang, *Phys. Rev. Lett.* **33**, 495 (1974).

¹³Y. Kawamura, K. Wakita, H. Asahi, and K. Kurumada, *Jpn. J. Appl. Phys.* **25**, L928 (1986).

¹⁴K. K. Choi, B. F. Levine, R. J. Malik, J. Walker, and C. G. Bethea, *Phys. Rev. B* **35**, 4172 (1987).

¹⁵R. E. Cavicchi, D. V. Lang, D. Gershoni, A. M. Sergent, H. Temkin, and M. B. Panish, *Phys. Rev. B* **38**, 13474 (1988).

¹⁶H. T. Grahn, H. Schneider, and K. V. Klizing, *Appl. Phys. Lett.* **54**, 1757 (1989).

¹⁷E. S. Snow, S. W. Kirchoefer, and O. J. Glembocki, *Appl. Phys. Lett.* **54**, 2023 (1989).